Influence of Crystallinity on the Fracture Toughness of Poly(lactic acid)/Montmorillonite Nanocomposites Prepared by Twin-Screw Extrusion

J. Gamez-Perez,[1] L. Nascimento,[1] J.J. Bou,[2] E. Franco-Urquiza,[1] O.O. Santana,[1] F. Carrasco,[3] M. Ll. Maspoch[1]

[1]*Centre Català del Plàstic (CCP), Universitat Politècnica de Catalunya, C/Colom 114, Terrassa 08222, Spain*
[2]*Departament d'Enginyeria Quimica, Universitat Politècnica de Catalunya, Av. Diagonal 647, Barcelona, Spain*
[3]*Department of Chemical Engineering, Universitat de Girona, Campus Montilivi, s/n. 17071 Girona (Spain)*

Received 15 April 2010; accepted 12 August 2010
DOI 10.1002/app.33191
Published online 5 November 2010 in Wiley Online Library (wileyonlinelibrary.com).

ABSTRACT: The aim of this work was to study the effect of crystallinity degree on the thermal, mechanical, and fracture properties of poly(lactic acid)/organomodified montmorillonite (PLA/OMMT) nanocomposites. Samples with two different compositions (0.5 and 2.5% weight OMMT in PLA) were prepared by melt mixing in a twin-screw extruder and injection molding. An annealing treatment was applied to increase the percentage of PLA crystallinity. The thermal behavior was analyzed by differential scanning calorimetry (DSC), and the mechanical properties were determined via tensile tests and the fracture behavior using the linear elastic fracture mechanics theory, using SENB specimens at low and high testing rates. Gel permeation chromatography (GPC) from granulates and injected specimens were also carried out, finding some polymer degradation during extrusion and injection processes. The results show a toughening effect of the nanocomposites on amorphous specimens but embrittlement on the annealed ones. © 2010 Wiley Periodicals, Inc. J Appl Polym Sci 120: 896–905, 2011

Key words: nanocomposites; fracture toughness; extrusion; annealing; poly(lactic acid); degradation

INTRODUCTION

Interest in biopolymers has increased in recent years due to concerns about preservation of the environment and the substitution of petrochemical polymers. The use of biodegradable polymers represents a potential route to solve the problems of plastic pollution and replacing, at least partially, polymers from petrochemical raw materials. In this context, Poly(lactic acid) (PLA) is one of the most promising polymers because it is biodegradable and made from renewable resources. Furthermore, PLA shows a good compromise between mechanical properties and processability.[1] However, other properties of PLA, such as poor thermal resistance and its low gas barrier, would limit the use of this biopolymer in certain applications.[2]

One potential solution for overcoming the constraints discussed above is the addition of nanosized fillers to form nanocomposites.[3] Because of the high aspect ratio of nanocomposites, mechanical, gas barrier, and fracture properties can be improved with very low reinforcement content, in the range of 1–5% weight.[4] Montmorillonites (MMT) are frequently used as fillers to produce nanocomposites because of their lamellar structure, with a thickness of about 1 nm. To improve the interaction of the polymer inside the clay galleries, and achieve complete exfoliation of the MMT, Na^+ cations are exchanged by more voluminous organic ones (alkylammonium cations), simultaneously increasing the stack space and the chemical compatibility between the hydrophilic clay surface and organophilic polymer chains. The more exfoliated is the clay in the matrix, the more reinforcement to mechanical stress and crack growth resistance can be obtained.[5,6]

Such organomodified montmorillonites (OMMT) have been commercially available for several years. Good dispersion of the clay to form nanocomposites can be obtained by melt-intercalation in a twin-screw extruder.[7] This may be the most convenient way to prepare nanocomposites when it is available, since it is a solvent-free process, which makes it attractive because it is more economic and environmentally friendly than *in situ* polymerization.[8] In recent years, several studies and reviews about PLA and nanofillers have been published.[9–11] However, there are only a few works that cover the fracture

Correspondence to: J. Gamez-Perez (jose.gamez@upc.edu).
Contract grant sponsor: Ministry of Education and Science of the Spanish Government; contract grant number: MAT2007-62450.

© 2010 Wiley Periodicals, Inc.

toughness of PLA and their composites[12,13], being unusual to find that information in the literature and how is its toughness affected by a second rigid phase.

The aim of this study was to understand the relationships produced by the addition of organomodified montmorillonite and variations on crystallinity on the mechanical, thermal, and fracture properties of injected PLA specimens.

EXPERIMENTAL

Materials

A commercial grade of PLA (PLA 2002D, Natureworks®), characterized by a relative density of 1.24, a D-monomer content of 4.25% and a residual monomer content of 0.3%[14] was used. The glass transition temperature (T_g) and the melting point temperature (T_m) of PLA 2002D are 58 and 153°C, respectively. The filler used was an organically modified montmorillonite (OMMT) (Cloisite® 30B, Southern Clay Products). The percentage of montmorillonite clay (MMT) in the organoclay was 70%, as assessed by calcination. The organic modifier of the OMMT is an organic cation $[N(CH_3)(C_2H_4OH)_2R]^+$, where R is an aliphatic radical with 16–18 carbon atoms.[15]

The first step of the compounding process was the production of the masterbatch, which was carried out using a corrotative twin-screw extruder (Collins, ZK 25, Germany) with a screw diameter of 25 mm and L/D ratio of 36. The screw speed was 80 rpm, the estimated residence time 150 s and the temperature profile ranged between 145 and 195°C. Since PLA is susceptible to hydrolytic degradation, the use of a dehumidifier (Piovan, DSN506HE) was necessary (80°C, for 3 h) prior to any type of processing. The PLA pellets and the OMMT were fed simultaneously into the extruder.

After granulation and drying, granulates were subjected to a second extrusion process using the same conditions to homogenize the compound. Subsequently, the exact composition of the masterbatch (nominally 4 wt % OMMT) was determined by calcination. The third step consisted of diluting the masterbatch with virgin PLA in the twin-screw extruder, to obtain two compounds with nominal compositions of 0.5 and 2.5 wt % OMMT.

ISO standard tensile specimens (type "I" according to ISO 527-1 1A) and prismatic bars with nominal dimensions 6.35 × 12.7 × 127 mm^3 were obtained by injection molding (Mateu and Sole, 440/90, Spain), with a temperature profile of 180, 200, and 210°C for the nozzle. The injection pressure was kept constant at 100 bars, and the mold temperature was set at 25°C.

To increase the crystalline fraction in the material, some of the injected pieces were annealed. According to Kawai et al.,[16] the growth rate of spherulites in PLA is maximum at a temperature between 100 and 125°C. For this reason, with the aim of obtaining the maximum crystalline fraction during annealing, this procedure was performed at 120°C for 6 h.

TABLE I
Materials Used in this Work, OMMT Content, and Brief Description

Materials	%MMT	%OMMT	Description
PLA-V			As received PLA pellets
PLA	–	–	PLA-V injection molded
PLA-0.5	0.32	0.46	Diluted nanocomposite (12% masterbatch) and injection molded
PLA-2.5	1.73	2.47	Diluted nanocomposite (67% masterbatch) and injection molded

The PLA specimens in this work are named according to their OMMT content (0.5 or 2.5) and thermal treatment (annealed samples are identified by the letter A). Table I describes the nomenclature used and the specific MMT content of the materials.

Characterization techniques

Transmission electron microscopy

Ultrathin transmission electron microscopy (TEM) samples were sectioned from the injected pieces with a Reichert 701701 ultra-microtome equipped with a diamond knife. Then, the ultrathin sections were observed in a high-resolution Hitachi 800MT transmission electron microscope, operating at 300 kV, to analyze the organoclay dispersion in the PLA matrix.

Scanning electron microscopy

The fractographic analysis was performed via scanning electron microscopy (SEM) using a JEOL JSM 6400. The micrographs were taken on the gold-sputtered fracture surface of postmortem specimens.

Melt flow index

Melt flow index (MFI) measurements were performed using a CEAST 6542/002 equipment, which determines MFI based on the ISO 1133/2001 standard. The weight used was 2.16 kg, and the temperature was 210°C.

Gel permeation chromatography

Samples were injected in an Agilent 1200 series LC system running at room temperature and using only the refractive index detector. Data were collected digitally using Ezchrom Software from Agilent Technologies (Santa Clara, CA). The separation column was a

Styragel HR5E from Waters (Milford, MA), and the mobile phase was 1,1,1,3,3,3-hexafluoro-2-propanol (HFIP) containing 6.8 g/L of sodium trifluoroacetate to prevent the polyelectrolyte effect; both compounds were acquired from Apollo Scientific (Manchester, UK). The flow rate was 0.5 mL/min. Twenty microliters were injected and the concentration of each sample was about 0.1% w/v. Calibration was performed using PMMA samples from Fluka (Buchs, Switzerland).

Differential scanning calorimetry

The thermal characterization was carried out by differential scanning calorimetry (DSC). The tests were performed on a Perkin–Elmer Pyris 1 equipped with a refrigeration system Intracooler Perkin 2P. The equipment was calibrated with indium and tin samples, and the tests were conducted under a nitrogen atmosphere, with a sample size of 10 mg encapsulated in aluminum pans. The samples were heated from 30 to 180°C and cooled down to 30°C with a heating/cooling rate of 10°C/min.

Mechanical characterization

The mechanical characterization was performed by tensile test according to the ISO 527-2 standard, using type 1A injected specimens and a universal testing machine (Galdabini Sun 2500) equipped with a 25-kN load cell. Deformations were measured with a video extensometer (Mintron OS-65D CCD video camera) in conjunction with Messphysik Windows-based software. The crosshead speed of the tests was 10 mm/min, and they were conducted at room temperature (23°C ± 2°C).

Fracture characterization

The linear elastic fracture mechanic (LEFM) was applied using single edge notched bend (SENB) specimens for mode I of the fracture toughness test. The specimen dimensions (12.7 × 63.5 × 6.35 mm^3) as well as the crack depth and strain rate of the tests were defined as indicated by the European Structural and Integrity Society (ESIS).[17] For low strain rates, the initial crack length (a_0) was 5.50 mm, whereas for the high strain rate a_0 varied between 2.00 and 6.75 mm. Prior to testing, the notches were sharpened with a single cut from a razor blade, as indicated in the ESIS protocol.[17]

The tests at low strain rate were performed using a universal testing machine (Galdabini Sun 2500) equipped with a 25-kN load cell. The crosshead speed of the test was 10 mm/min, and the tests were conducted at room temperature (23°C ± 2°C).

The tests at high strain rate were carried out using a Charpy (Ceast) pendulum equipped with an instrumented pendulum hammer of 34.64 g of effective mass. The impact velocity was set to 1 m/s, and tests were performed at room temperature (23°C ± 2°C). The fracture toughness was calculated using the following equation[17]:

$$K_{IC} = f\frac{P_c}{BW^{1/2}} \quad (1)$$

where P_c is the maximum load point, and B and W are the thickness and width of the specimens, respectively. The geometrical correction factor, f, is given as a function of a/W, where a is the initial crack length.[17]

RESULTS AND DISCUSSION

Morphological characterization

The exfoliation of the silicate layer was analyzed by means of TEM. Figure 1(a,c) show some microsized clay aggregates along with exfoliated clay layers. PLA-2.5 seemed to have more aggregates than PLA 0.5. Examination at higher magnifications, as in Figure 1(b,d), clearly revealed the exfoliated structure of the composites.

The mixing process of the clays and the PLA matrix involves a processing step that may have a strong influence on the final properties of the composites. As it is well known, thermomechanical stress can induce degradation of PLA while it is being processed.[18,19] Such degradation will cause variations on the PLA molecular structure and average molecular weight. Table II summarizes the different parameters characterizing the molecular mass distributions obtained from GPC. As shown in Table II, there is a significant decrease in the average molecular weight of injected PLA specimens, compared to that of the virgin PLA pellets (PLA-V). Indeed, the nanocomposites show a more pronounced reduction in the average molecular weight than PLA, which can be attributed to the preparation of the masterbatch with two passes through the twin-screw extruder and the additional dilution step, also in the twin-screw extruder. This trend was also observed for the values of M_z and is consistent with previous work of our group on the reprocessing of PLA in a single-screw extruder.[19] These data are also consistent with the MFI values, also shown in Table II, with an increase in the MFI as the average molecular weight decreased. Furthermore, as the OMMT was added, there was a considerable increase in the MFI values, which could indicate a plasticizing effect of the organomodified clays.

The number average molecular weight, M_n, however, showed a curious deviation from this trend, with an increase in M_n for PLA-2.5, which contained

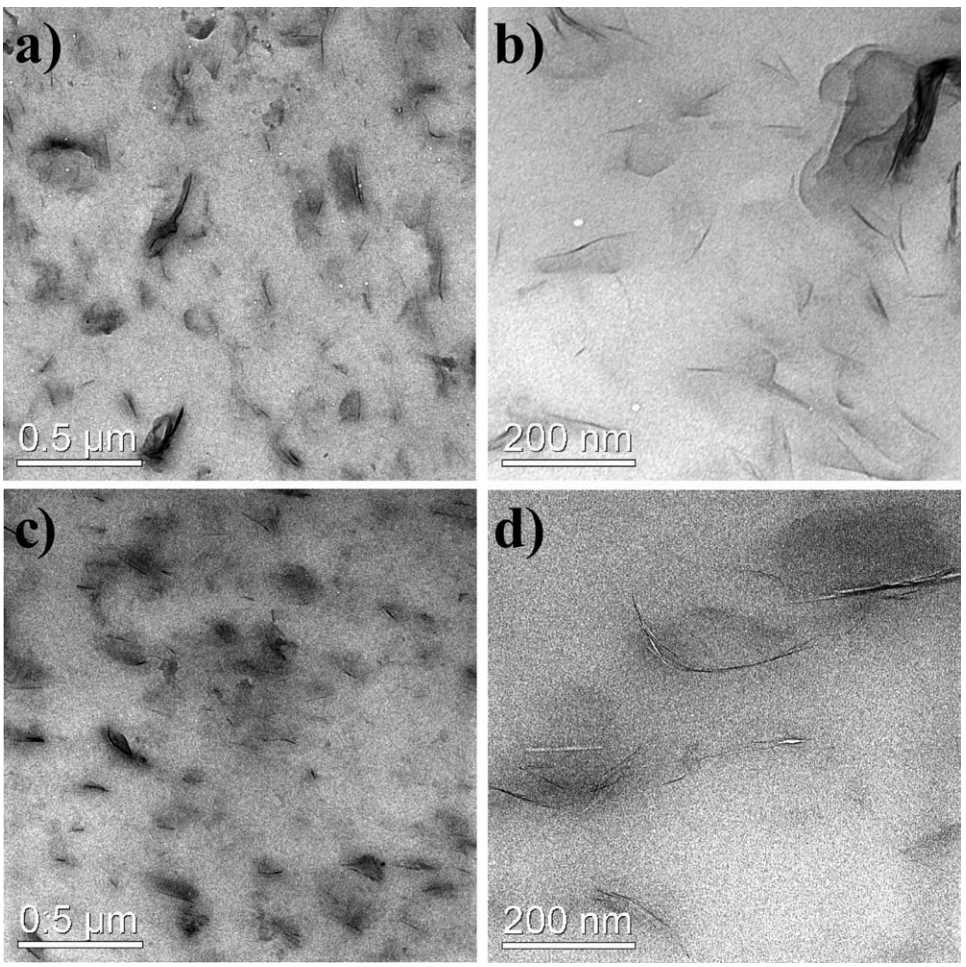

Figure 1 TEM micrographs of PLA nanocomposites: PLA 0.5 (a and b) and PLA-2.5 (c and d).

almost 65% of the masterbatch. The loss of molecular weight with high clay loadings could be also the result of some hydrolysis, since clay has associated water, aminolysis by the organic modifiers or by chain scission/transterification caused by thermal and shear stress.[20,21] In any case, the rupture of the chains would be more plausible statistically in longer chains than in shorter ones, thus leading to a more pronounced reduction in M_z and M_w than in M_n. Assuming that the longer chains are split into "smaller" ones, the resulting fragments may have a larger size than the average M_n, thus leading to an increase in this value and resulting in homogenization of the molecular weight distribution and a decrease in the polydispersity (PD) index. The interesting change in PD looks like the same came to equilibrium, at 2.0, in agreement with the thermal degradation model proposed by Yu et al.[22]

Thermal behavior

Figure 2 shows the DSC thermograms corresponding to the first heating step of the samples. PLA showed an endothermic peak close to the glass transition temperature (T_g = 63°C), corresponding to an enthalpy relaxation phenomenon associated with polymer physical aging.[23] This aging is characterized by a specific volume reduction in the amorphous phase,

TABLE II
Molar Mass Data from GPC and MFR Analysis

Sample	M_n (Dalton)	M_w (Dalton)	M_z (Dalton)	PD	Mp* (Dalton)	MFR (g/10 min)
PLA-V	76,800	216,500	408,400	2.82	205,300	7.0
PLA	62,600	189,500	382,200	3.03	155,500	7.4
PLA-0.5	53,400	175,000	386,500	3.28	155,800	18
PLA-2.5	67,800	134,200	249,000	1.98	87,500	24.4

Mp* peak mass from GPC curve.

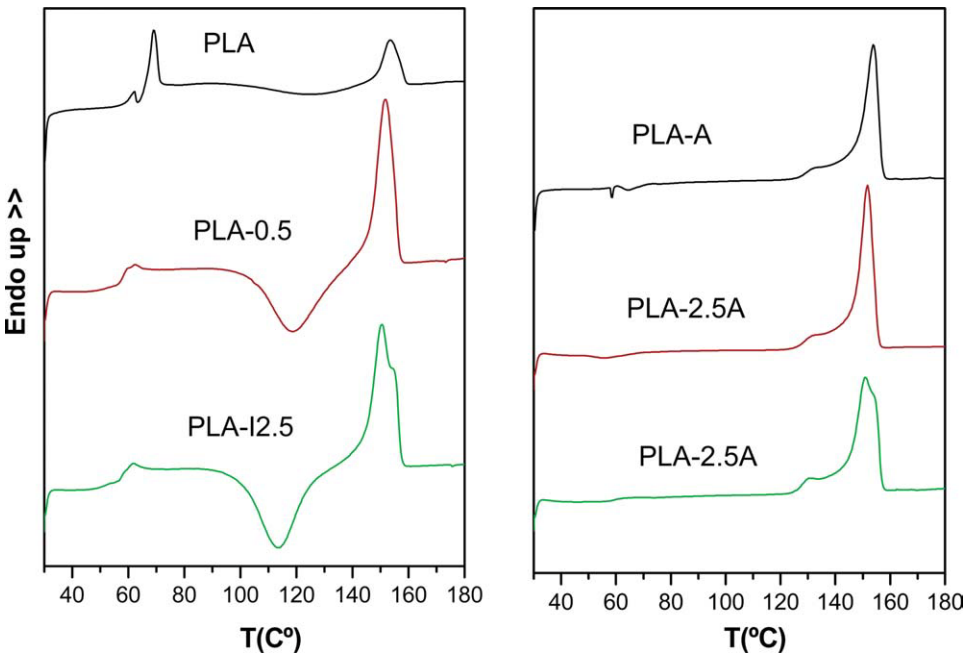

Figure 2 DSC first heating scan curves of PLA and nanocomposites before (a) and after (b) the annealing treatment. [Color figure can be viewed in the online issue, which is available at wileyonlinelibrary.com]

and it takes place at temperatures below T_g. In Figure 2(a), it can be seen that the intensity of that peak was minimized by the addition of the OMMT, which suggests that the addition of the organoclay hampers this aging phenomenon, maybe promoted by the interactions between the organomodifier and the polymer. On the other hand, the T_g corresponding to nanocomposites (shown in Table II) are also lower than the pure PLA, indicating that that polymer chains in nanocomposites have more free volume than in pure PLA, which could be a consequence of the molecular weight loss during processing.

Regarding the thermograms of the nonannealed nanocomposites in Figure 2(a), an intense exothermic peak can be observed. Such a peak was attributed to a cold crystallization phenomenon[24] and could be influenced by the presence of the nanofillers, as suggested by other authors.[25] In addition, due to PLA degradation, there was an increase in chain mobility, which also promotes this phenomenon.[19,26] Finally, an endothermic peak can be seen at 145°C, which was associated with the melting of the crystalline fraction.

The degree of crystallinity (X_c) of the different samples was calculated from the first heating scan, subtracting the cold crystallization enthalpy (ΔH_{cc}) from the melting enthalpy (ΔH_f), as indicated in the following equation:

$$X_c = \left(\frac{\Delta H_f - \Delta H_{cc}}{\Delta H_0}\right) \cdot 100\% \qquad (2)$$

where ΔH_0 corresponds to an ideal melting enthalpy of 93 kJ/kg.[27] The degree of crystallinity (X_c), the glass transition temperatures (T_g), and the melting temperatures (T_m) of the injected specimens are summarized in Table II. On the basis of the GPC values, it was concluded that the addition of the OMMT through three processing steps (masterbatch, homogenization, and dilution) led to degradation of the PLA with chain scissions. This degradation, generating smaller chains, could have a plasticizer-like effect inside the material, since the shorter chains have higher mobility and the increase in chain-ends also increases the free volume of the system.[19] This reasoning is consistent with the DSC data, which showed a significant decrease in the glass transition temperature of the nanocomposites and a faster cold crystallization phenomenon.[26,28]

The thermogram of the PLA-2.5 sample shows a double melting peak, which was not observed in PLA or PLA-0.5 samples. Such peak can be a consequence of the influence that the nanoclays have on the crystallization kinetics and structure, as reported by several authors.[29–31]

After the annealing thermal treatment [Fig. 2(b)] there were no peaks associated to the cold crystallization phenomenon in the thermograms, but instead there were larger and defined melting peaks. As expected, the degree of crystallinity increased after annealing, finding a raise of X_c of about 30%. These values are summarized in Table II. The melting peaks contained a shoulder at lower temperatures, which suggests the occurrence of two crystalline populations, named α and α′, as suggested by Zhang et al.,[32] which could be simultaneously promoted at the annealing temperature of 120°C. The annealed

TABLE III
DSC Parameters for the Thermal Transitions Observed in PLA and Nanocomposites

Materials	T_g (°C)	T_m (°C)	X_c (%)	X_c (%)-A
PLA	65.9	148.5	0.4	32.3
PLA-0.5	59.7	149.8	3.9	35.4
PLA-2.5	58.8	147.3	2.2	35.6

A, Annealed specimens.

samples did not show any sign of cold crystallization, indicating that the materials had already reached their maximum degree of crystallinity.

Mechanical characterization

In general, PLA and nanocomposites showed very little plastic deformation before their catastrophic failure, at low deformation values, without the formation of a defined neck. Table III summarizes the main parameters obtained from the stress-strain curves.

In the case of nonannealed specimens, the addition of OMMT did not cause any significant variation in the stiffness of the specimens, with similar Young Modulus values for PLA and the composites. Even though montmorillonite can provide stiff reinforcement for PLA, it should be noted that it is present at very low concentrations. On the other hand, plastic deformation occurs at lower stress (σ_y) and strain (ε_y) levels than in PLA, which indicates that OMMT promotes plastic deformation. This was also demonstrated in the values of deformation at the break point (ε_b), with composites showing higher values than those obtained for PLA.

Comparing these values with previous studies in which PLA reprocessing was analyzed[19,26] such increase in plastic deformation cannot be explained only by taking into account the polymer chain degradation occurring during the preparation of the OMMT masterbatch. The presence of the clay organomodifier must also be taken into account, comprising about 30% in weight of the OMMT and potentially acting as a plasticizer in the PLA matrix. These two factors can explain the increase in the polymer chain free volume, thus resulting in lower σ_y and ε_y values and higher overall plastic deformation, in agreement with the previous DSC results, in which a decrease in T_g values as the OMMT increased was found (Table III).

The annealing treatment led to an increase in stiffness and a decrease in plastic deformation in all cases, as can be deduced from the data presented in Table IV. Nanocomposites failed before reaching the yield strength of the material, during the initial linear portion of the stress–strain curve. Furthermore, as the OMMT content increased, the strain at the break point decreased.

TABLE IV
Main Mechanical Properties of Unfilled PLA and Nanocomposites (Young Modulus, Yield Strength, and Strain at Break Point)

Materials	E (GPa)	σ_y (MPa)	ε_y (%)	ε_b (%)
PLA	3.7 ± 0.2	62.0 ± 0.2	1.92 ± 0.04	4.0 ± 0.08
PLA-0.5	3.7 ± 0.2	58.1 ± 0.2	1.84 ± 0.02	5.7 ± 0.8
PLA-2.5	3.9 ± 0.2	55.6 ± 0.1	1.63 ± 0.06	11 ± 2
PLA-A	4.1 ± 0.1	69.1 ± 1.5	1.91 ± 0.05	3.3 ± 0.3
PLA-0.5A	4.2 ± 0.2	65.2 ± 1.6[a]	[a]	1.63 ± 0.04[a]
PLA-2.5A	4.5 ± 0.1	54.1 ± 2.0[a]	[a]	1.22 ± 0.06[a]

[a] Failure before yielding.

The increase in stiffness and yield strength can be related to the presence of the more rigid crystalline phase (about 30%), which was promoted by the annealing treatment. This increase in X_c was accompanied by a decrease in the chain mobility of the amorphous phase, resulting in a lower ability to deform plastically than in the nonannealed specimens. The failure of the annealed nanocomposites before yielding can be attributed to the presence of some OMMT aggregates, which could act as stress concentrators,[33] combined with the reduction in chain mobility and entanglement density.[34]

Fracture characterization

As mentioned previously, the fracture behavior of PLA was evaluated at low and high strain rates. In all cases, the materials presented the typical brittle behavior of polymers tested below their T_g, allowing the application of the linear elastic fracture mechanics (LEFM) to characterize the fracture toughness (K_{IC}), according to the ESIS protocol.[17]

Figure 3 summarizes the K_{IC} values of the materials at low strain rates (10 mm/min). It can be seen

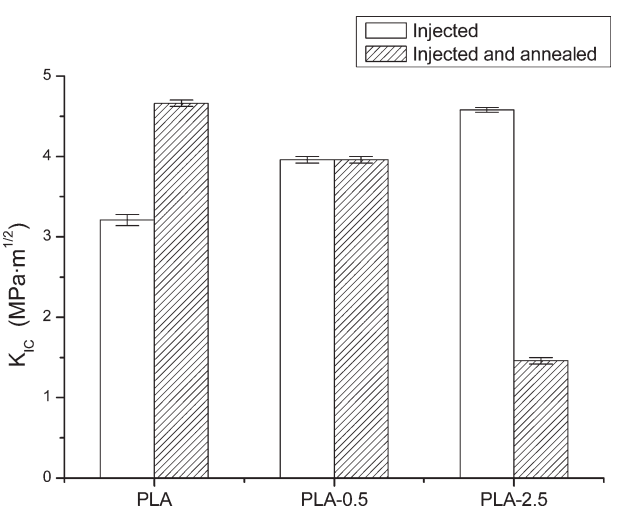

Figure 3 K_{IC} values of PLA and nanocomposites tested at low strain rate (10 mm/min).

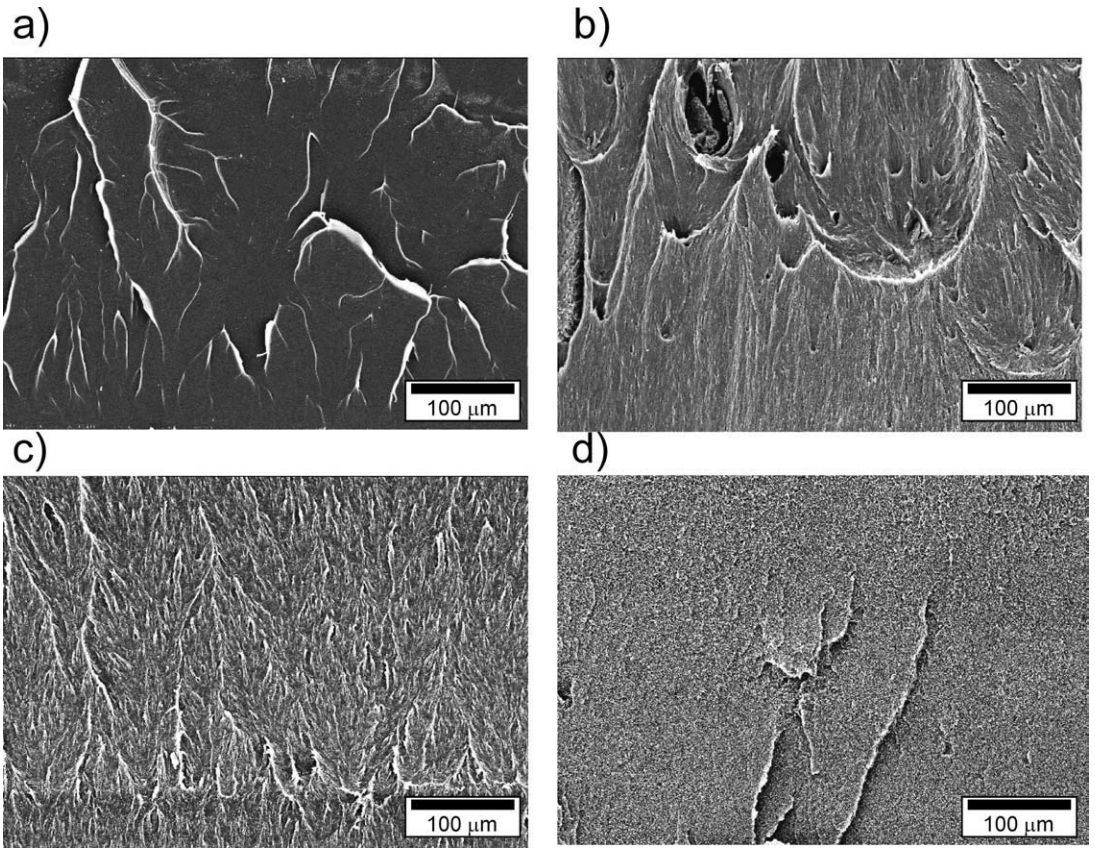

Figure 4 SEM micrographs of postmortem SENB samples tested at low testing rate (10 mm/min), near the notch: (a) PLA, (b) PLA-2.5, (c) PLA-A, and (d) PLA-2.5-A. The direction of crack propagation is from bottom to top.

that the fracture toughness increased as the OMMT content increased in nonannealed samples, with an improvement of 40% in the case of PLA-2.5. This was consistent with the mechanical results, in which a gradual increase in the plastic deformation occurred when the OMMT content was increased. However, as the matrix M_w decreases with the clay content, and given that the PLA is in an amorphous state, a decrease in the fracture toughness should be expected due to the lower entanglement density.[34] So, to explain such trend, two hypotheses can be considered: the increase of chain mobility and interactions between the polymer matrix and the OMMT. The increase of the chain mobility is a direct consequence of the PLA degradation, which comes with an increase in the free volume of the chains, as observed in DSC experiments. This results in a higher ability to flow, as observed in tensile tests with higher deformations at break. On the other hand, Giannelis and coworkers[35] have shown that an increase in toughness can be achieved by addition of small amounts of MMT, which provide a physically crosslinked structure with stress transfer mechanism between polymer domains. Such network could be counterbalancing the loss of entanglement density, resulting in the improvement of the fracture toughness. Such reinforcement mechanism, nevertheless, requires a certain mobility of the polymer matrix.[36]

With respect to the annealed samples, PLA-A showed an increase of 40% in K_{IC} values. This trend can be related to the mechanical tests, where PLA-A showed a higher yield strength and similar deformation at yield than PLA. However, by combining the effect of the OMMT and annealing, instead of finding a synergetic effect in terms of fracture toughness resistance for the annealed nanocomposites, a severe decrease in K_{IC} is found as the OMMT content increases. Since the mobility of the polymer is even more restricted than in the case of the amorphous systems, due to the crystalline phase, the nanoparticles cannot increase the toughness of the composites.[36] The nanoparticles act, in these cases, like conventional fillers, initiating crack formation and fracture.

The fracture analysis of postmortem samples, carried out by SEM, showed the development of different fracture topologies, depending on the OMMT content and/or the annealing treatment (Fig. 4). The nonannealed specimens showed some stretched crests in the fractured surface and no signs of extensive plastic deformation. Such crests could have been originated during craze growth, between the

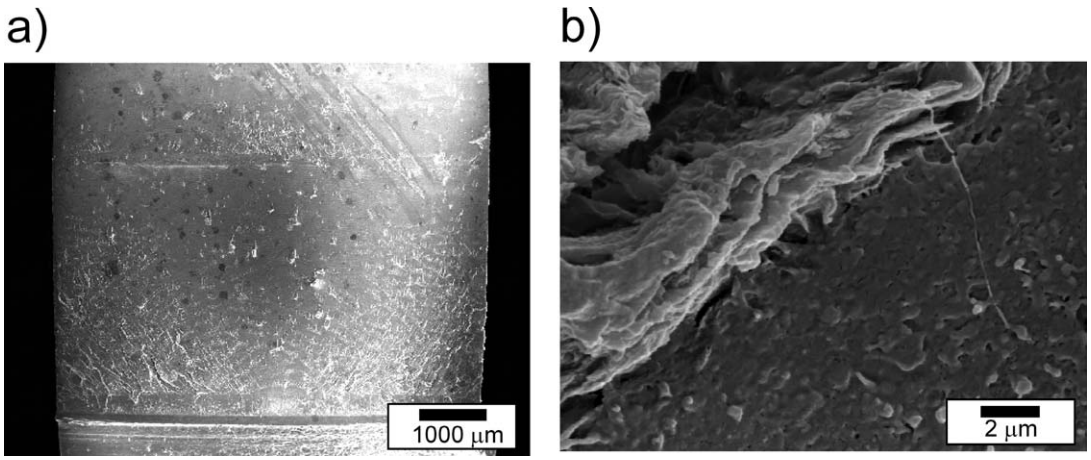

Figure 5 Aggregates on the fracture surface of postmortem impact specimens of PLA-2.5: (a) surface overview and (b) detail of an aggregate at ×7000.

craze faces. On the other hand, there is some white iridescence in the fracture surface, suggesting a multiple crazing phenomenon. The length of the crests would indicate that the crazes were stabilized during their growth, visible by the development of small fibrils on the fractured surface, increasing in number as the OMMT content increased [Fig. 4(a,b)]. This stabilization would have allowed the generation of multiple crazes in different planes.

After annealing, such fibrils were observed only in pure PLA [Fig. 4(c)] but not in the nanocomposites [Fig. 4(d)] where the crazes were not stabilized.

Summarizing, the evaluation of the fracture toughness of PLA/OMMT nanocomposites requires taking into account several factors, some of them acting in opposite directions:

(a) The reduction of entanglement density in the amorphous phase, due to polymer degradation (decrease on toughness).
(b) A plasticizing effect on the polymer matrix, induced by degradation and/or by clay organomodifiers (increase on toughness).
(c) The interactions between the PLA matrix and nanoclays, which can lead to a physical crosslinked network (increase on toughness).
(d) The presence of OMMT aggregates, which could act as stress concentrators[33] (decrease on toughness).

In the case of nanocomposites without thermal treatment, factors (b) and (c) would lead to enhanced fracture toughness, resulting in an increase in K_{IC} with the increase in OMMT content. In the case of annealed nanocomposites, the reduction chain mobility induced by crystallization, in addition to the presence of OMMT aggregates and the reduction in molecular weight, led to a reduction in the fracture toughness compared to that of pure PLA.

The presence of clay aggregates was more easily observed on the fracture surface of impact-tested specimens, as in Figure 5(a), where they are present across the whole surface. A close-up of these aggregates is presented in Figure 5(b), where the clay layers, verified by elemental analysis, can also be identified. Indeed, Figure 5(b) also shows good compatibility between the clay aggregates and the polymer matrix.

Even though the same arguments considered in low strain rate fracture tests could also be used to analyze the K_{IC} values obtained at the impact rate (1 m/s), the values obtained (summarized in Fig. 6), were quite similar among them, due to the effect of the high testing speed, which inhibits the ability of the polymer to deform plastically. The fracture toughness of the samples was, in any case, always lower than the values obtained at low strain rates (Fig. 3).

The fractographic analysis, however, showed that the fracture mechanisms differ depending on the annealing treatment and the presence of OMMT.

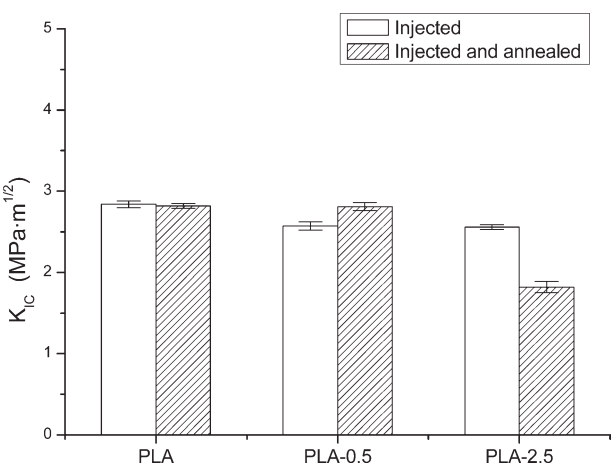

Figure 6 K_{IC} values of PLA and nanocomposites tested at impact strain rate (1 m/s).

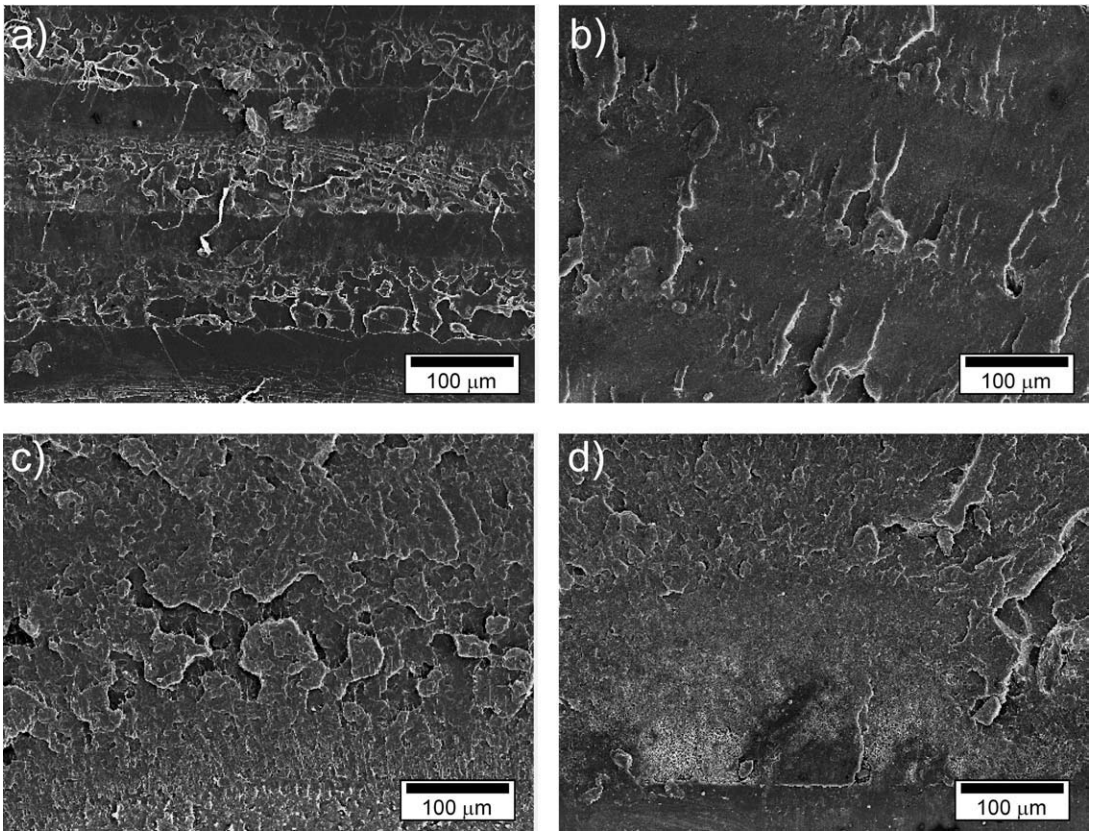

Figure 7 SEM micrographs of postmortem SENB samples tested at impact rate (1 m/s), near the notch: (a) PLA, (b) PLA-2.5, (c) PLA-A, and (d) PLA-2.5-A. The direction of crack propagation is from bottom to top.

Figure 7 shows such differences in some fracture microphotographs. The nonannealed specimens [Fig. 7(a,b)] showed a typical mackerel pattern, like those that can be found in amorphous polymers tested at high rates.[37] Nevertheless, the nanocomposites [Fig. 7(b)] had a smoother surface than PLA, with some aggregates on the fractured surface that could induce premature failure, in agreement with the K_{IC} values. With regards the annealed specimens [Fig. 7(c,d)], the fracture surface of PLA and the nanocomposites had in common a rough surface with multiple cleavage planes and no evidence of plastic flow. In this case, it seems that it is the role of the OMMT aggregates as stress concentrators that makes a difference in the low impact fracture values of annealed nanocomposites.

CONCLUSIONS

The TEM micrographs showed that the PLA/OMMT composites were exfoliated, even though a significant number of aggregates were also observed. GPC data indicated that the masterbatch preparation induced some thermomechanical degradation, with a decrease in the molecular weight of the longest chains. On the basis of the DSC thermograms, it can be concluded that the nanocomposites showed higher chain mobility and that the thermal treatment led to a considerable increase in the degree of crystallinity.

The mechanical properties and the fracture behavior were predominantly affected by four factors:

(a) the degree of crystallinity (X_c)
(b) the matrix degradation (plasticizing effect and decrease in entanglements)
(c) the nature of the clay organomodifier (interaction with the matrix and/or possible plasticizing effect)
(d) the presence of clay aggregates in the matrix

In the case of nonannealed specimens, the nanocomposites improved the fracture toughness of PLA without reducing its stiffness. However, when the specimens were annealed, the presence of aggregates and limited chain mobility were limiting factors, reducing their performance in tensile and fracture tests. This works highlights the benefits/disadvantages of the use of nanocomposites, depending on whether the application involves a crystallized specimen or an amorphous one.

References

1. Lim, L. T.; Auras, R.; Rubino, M., Progr Polym Sci 2008, 33, 820.
2. Fukushima, K.; Kimura, Y. Polym Int 2006, 55, 626.

3. Ray, S. S.; Yamada, K.; Okamoto, M.; Fujimoto, Y.; Ogami, A.; Ueda, K. Polymer 2003, 44, 6633.
4. Alexandre, M.; Dubois, P. Mater Sci Eng R-Reports 2000, 28, 1.
5. Chin, I. J.; Thurn-Albrecht, T.; Kim, H. C.; Russell, T. P.; Wang, J. Polymer 2001, 42, 5947.
6. Giannelis, E. P. Adv Mater 1996, 8, 29.
7. Pluta, M.; Galeski, A.; Alexandre, M.; Paul, M. A.; Dubois, P. J Appl Polym Sci 2002, 86, 1497.
8. Ray, S.; Okamoto, M. Progr Polym Sci (Oxford) 2003, 28, 1539.
9. Di, Y. W.; Iannace, S.; Di Maio, E.; Nicolais, L. J Polym Sci Part B: Polym Phys 2005, 43, 689.
10. Okamoto, M., Biodegradable Polymer/Layered Silicate Nanocomposites: A Review, in Handbook of Biodegradable Polymeric Materials and Their Applications, S.K. Mallapragada and B. Narasimhan, Editors. 2005, American Scientific Publishers: Ames, USA. p. 1–45.
11. Raquez, J. M.; Narayan, R.; Dubois, P. Macromol Mater Eng 2008, 293, 447.
12. Yuzay, I. E.; Auras, R.; Selke, S. J Appl Polym Sci 2010, 115, 2262.
13. Park, S. D.; Todo, M.; Arakawa, K. J Mater Sci 2004, 39, 1113.
14. NatureWorks® PLA Polymer 2002D. Data Sheet, Natureworks LLC, http://www.natureworksllc.com
15. Cloisite® 30B Typical Physical Properties Bulletin, Southern Clay Products. 2006. http://www.scprod.com/.
16. Kawai, T.; Rahman, N.; Matsuba, G.; Nishida, K.; Kanaya, T.; Nakano, M.; Okamoto, H.; Kawada, J.; Usuki, A.; Honma, N.; Nakajima, K.; Matsuda, M. Macromolecules 2007, 40, 9463.
17. Pavan, A., Determination of Fracture Toughness (GIC and KIC) at Moderately High Loading Rates, in Fracture Mechanics testing methods for polymers, adhesives and composites, D.R. Moore, A. Pavan, and J.G. Williams, Editors. 2001, Elsevier Science, Ltd.: Oxford. p. 27–58.
18. Taubner, V.; Shishoo, R. J Appl Polym Sci 2001, 79, 2128.
19. Carrasco, F.; Pages, P.; Gamez-Perez, J.; Santana, O. O.; Maspoch, M. L. Polym Degrad Stabil 2010, 95, 116.
20. Kopinke, F. D.; Remmler, M.; Mackenzie, K.; Möder, M.; Wachsen, O. Polym Degrad Stabil 1996, 53, 329.
21. Wang, Y.; Steinhoff, B.; Brinkmann, C.; Alig, I. Polymer 2008, 49, 1257.
22. Yu, H.; Huang, N.; Wang, C.; Tang, Z. J Appl Polym Sci 2003, 88, 2557.
23. Brunacci, A.; Cowie, J. M. G.; McEwen, I. J. J Chem Soc Faraday Trans 1998, 94, 1105.
24. Sics, I.; Ezquerra, T. A.; Nogales, A.; Denchev, Z.; Alvarez, C.; Funari, S. S. Polymer 2003, 44, 1045.
25. Pluta, M. J Polym Sci Part B: Polym Phys 2006, 44, 3392.
26. Nascimento, L.; Gamez-Perez, J.; Santana, O. O.; Velasco, J. I.; Maspoch, M. L. J Polym Environ, to appear.
27. Fischer, E. W.; Sterzel, H. J.; Wegner, G. Colloid Polym Sci 1973, 251, 980.
28. Pluta, M.; Jeszka, J. K.; Boiteux, G. Eur Polym J 2007, 43, 2819.
29. Pluta, M.; Galeski, A. J Appl Polym Sci 2002, 86, 1386.
30. Nam, J. Y.; Ray, S. S.; Okamoto, M. Macromolecules 2003, 36, 7126.
31. Ogata, N.; Jimenez, G.; Kawai, H.; Ogihara, T. J Polym Sci Part B: Polym Phys 1997, 35, 389.
32. Zhang, J. M.; Duan, Y. X.; Sato, H.; Tsuji, H.; Noda, I.; Yan, S.; Ozaki, Y. Macromolecules 2005, 38, 8012.
33. Jiang, L.; Zhang, J. W.; Wolcott, M. P. Polymer 2007, 48, 7632.
34. Kramer, E. J. J Mat Sci 1979, 14, 1381.
35. Xu, W.; Raychowdhury, S.; Jiang, D. D.; Retsos, H.; Giannelis, E. P. Small 2008, 4, 662.
36. Shah, D.; Maiti, P.; Jiang, D. D.; Batt, C. A.; Giannelis, E. P. Adv Mater 2005, 17, 525.
37. Sanchez-Soto, M.; Gordillo, A.; Maspoch, M. L.; Velasco, J. I.; Santana, O. O.; Martinez, A. B. Polym Bull 2002, 47, 587.